Erni, B. (1986) *Biochemistry 25*, 305–312.
Erni, B., & Zanolari, B. (1986) *J. Biol. Chem. 261*, 16398–16403.
Erni, B., Zanolari, B., & Kocher, H. P. (1987) *J. Biol. Chem. 262*, 5238–5247.
Grenier, F. C., Waygood, E. B., & Saier, M. H., Jr. (1985) *Biochemistry 24*, 47–51.
Hunt, S. (1985) in *Chemistry and Biochemistry of the Amino Acids* (Barrett, G. C., Ed.) pp 376–398, Chapman and Hall, London.
Kalbitzer, H. R., Deutscher, J., Hengstenberg, W., & Rösch, P. (1981) *Biochemistry 20*, 6178–6185.
Lee, C. A., & Saier, M. H., Jr. (1983) *J. Biol. Chem. 258*, 10761–10767.
Manayan, R., Tenn, G., Yee, H. B., Desai, J. D., Yamada, M., & Saier, M. H., Jr. (1988) *J. Bacteriol. 170*, 1290–1296.
Marti, T., Rösselet, S. J., Titani, K., & Walsh, K. A. (1987) *Biochemistry 26*, 8099–8109.
Pas, H. H., & Robillard, G. T. (1988) *Biochemistry* (in press).
Pas, H. H., ten Hoeve-Duurkens, R. H., & Robillard, G. T. (1988) *Biochemistry* (in press).
Pigiet, V., & Conley, R. R. (1978) *J. Biol. Chem. 253*, 1910–1920.
Post, R. L., & Kume, S. (1973) *J. Biol. Chem. 248*, 6993–7000.
Reiche, B., Frank, R., Deutscher, J., Meyer, N., & Hengstenberg, W. (1988) *Biochemistry* (in press).
Robillard, G. T., & Konings, W. N. (1981) *Biochemistry 20*, 5025–5032.
Robillard, G. T., & Beechey, R. B. (1986) *Biochemistry 25*, 1346–1354.
Robillard, G. T., & Blaauw, M. (1987) *Biochemistry 26*, 5796–5803.
Robillard, G. T., Dooijewaard, G., & Lolkema, J. S. (1979) *Biochemistry 18*, 2984–2989.
Rogers, M. J., Oghi, T., Plumbridge, J., & Söll, D. (1988) *Gene 62*, 197–207.
Roossien, F. F., & Robillard, G. T. (1984) *Biochemistry 23*, 211–215.
Roossien, F. F., Brink, J., & Robillard, G. T. (1983) *Biochim. Biophys. Acta 760*, 185–187.
Saier, M. H., Jr., Feucht, B. U., & Mora, M. K. (1977) *J. Biol. Chem. 252*, 8899–8907.
Saier, M. H., Jr., Grenier, F. C., Lee, A. C., & Waygood, E. B. (1985) *J. Cell. Biochem. 27*, 43–56.
Saier, M. H., Jr., Yamada, M., Erni, B., Suda, K., Lengeler, J., Ebner, R., Argos, P., Rak, B., Schnetz, K., Lee, C. A., Stewart, G. C., Breidt, F., Jr., Waygood, E. B., Peri, K. G., & Doolittle, R. F. (1988) *FASEB J. 2*, 199–208.
Sikkema, K. D., & O'Leary, M. H. (1988) *Biochemistry 27*, 1342–1347.
Stephan, M. M., & Jacobson, G. R. (1986) *Biochemistry 25*, 8230–8234.
Sutrina, S. L., Waygood, E. B., Grenier, F. C., & Saier, M. H., Jr. (1987) *J. Biol. Chem. 262*, 2636–2641.
Weigel, N., Powers, D. A., & Roseman, S. (1982) *J. Biol. Chem. 257*, 14499–14509.
Yamada, M., & Saier, M. H., Jr. (1987) *J. Biol. Chem. 262*, 5455–5463.

Helically Organized Macroaggregates of Pigment–Protein Complexes in Chloroplasts: Evidence from Circular Intensity Differential Scattering†

Gyozo Garab,‡ Sam Wells,§ Laura Finzi, and Carlos Bustamante*,‖
Chemistry Department, The University of New Mexico, Albuquerque, New Mexico 87131
Received May 3, 1988; Revised Manuscript Received June 7, 1988

ABSTRACT: Angle dependence of circular intensity differential scattering (CIDS) and of nonpolarized scattering was determined in isolated spinach chloroplasts at 514.5 nm. CIDS between 0° and 170° was independent of the nonpolarized scattering and showed intense lobes of alternating signs, exhibiting the negative and positive maxima around 15° and 70°, respectively. These results provide experimental evidence for the existence of large helically organized macroaggregates of pigment–protein complexes in thylakoid membranes. Modeling of the CIDS data by a simple helical array of uniaxial polarizable groups suggests that the chiral structure is left-handed with pitch and radius of the order of 385 nm.

In all photosynthetic organisms, the light-harvesting pigment–protein complexes and the reaction centers form a cooperative highly organized and regulated energy transfer and trapping system. The primary structure, the orientation of pigment molecules with respect to molecular axes, embedding of complexes in the membrane, and the three-dimensional model are known for many pigment–protein and reaction center complexes [for recent reviews, see Michel and Deisenhofer (1986), Zuber et al. (1987), Breton and Nabedryk (1987) and Garab et al. (1987)]. Our knowledge about the supramolecular organization of complexes is derived mainly from freeze–fracture (–etch) microscopy (Staehelin, 1986). The micrographs, however, do not carry information about possible interactions between different complexes or particles.

Circular intensity differential scattering (CIDS)[1] is a newly emerging structure-analysis technique (Tinoco et al., 1983).

† This work has been supported by grants from the National Institutes of Health, GM 32543 to C.B., and the National Science Foundation, DMB-8609654 and DMB-8501024 to C.B. Additional support was provided by the Center of High Tech & Materials of UNM.
* To whom correspondence should be addressed.
‡ On leave from the Institute of Plant Physiology, Biological Research Center, Hungarian Academy of Sciences, Szeged H-6701, Hungary.
§ Present address: Department of Applied & Engineering Physics, Cornell University, New York, NY 14853.
‖ Alfred P. Sloan Fellow and Searle Scholar.

[1] Abbreviations: CD, circular dichroism; CIDS, circular intensity differential scattering $[(I_L - I_R)/(I_L + I_R)$, where I_L and I_R are the intensities scattered upon illumination with left and right circularly polarized light, respectively]; LHC II, chlorophyll *a*/*b* light harvesting pigment–protein complex of photosystem II.

0006-2960/88/0427-5839$01.50/0

This technique arises from the ability of long-range chiral macrodomains, whose dimensions are a sizable fraction of the wavelength of the light employed, to interact preferentially with one or the other circular polarizations of light.

The CIDS ratio is given by

$$\mathrm{CIDS}(\theta) = [I_L(\theta) - I_R(\theta)]/[I_L(\theta) + I_R(\theta)]$$

where $I_{L,R}(\theta)$ denotes the intensity scattered by the sample at angle θ for incident left (L) and right (R) circularly polarized light. The theory of CIDS has been developed (Bustamante et al., 1980, 1983, 1985), and this sensitive technique has been applied in various biological and physical systems, such as sperm heads (Maestre et al., 1982; Wells et al., 1986), bacteriophage (Tinoco et al., 1983), Chinese hamster cells (Maestre et al., 1985), and cholesteric liquid crystals (Hall et al., 1985).

Recent circular dichroism studies in chloroplasts indicate that circular differential scattering plays an important role in defining the static and dynamic CD characteristics of thylakoid membranes (Garab et al., 1988a,b). Hence, CIDS is potentially a specific, nondestructive technique for studying the supramolecular organization of pigment–protein complexes in native photosynthetic membranes. In this paper, we report the results of the first systematic angle-dependent CIDS measurements in chloroplasts. In agreement with the theoretical predictions for helically organized macrodomains [cf. Bustamante et al. (1980, 1982)], we found that (i) CIDS, as a function of the scattering angle, shows intense lobes with alternating signs and (ii) this function is independent of the nonpolarized scattering. These results provide experimental evidence for the existence of helically organized macrodomains in chloroplast thylakoid membranes. The results also suggest that a considerable fraction of the pigment–protein complexes is assembled into large helically organized macroaggregates.

Experimental Procedures

Chloroplast thylakoid membranes [class C chloroplasts (Hall, 1972)] were prepared as previously described (Chylla et al., 1987). The reaction buffer, 100 mM sorbitol, 20 mM KCl, 5 mM $MgCl_2$, and 30 mM tricine/KOH, pH 7.8, was passed through a bacterial filter to avoid any contamination that could contribute to the CIDS signal.

The CIDS instrument used in this study has been described in detail (Katz et al., 1984; Wells et al., 1986). The incident intensity of the 514.5-nm laser beam of 3-mm diameter of the Ar ion laser was adjusted to about 20–40 mW. At these powers, the light caused on noticeable effects on the integrity of the sample. The measurements in the forward and backward directions, between 0° and 30° and 150° and 170°, respectively, were carried out in a rectangular fused silica cell of 1-cm optical path length. (The scattering angles were corrected for the refractive index of the cuvette.) The angle dependence of scattering between 20° and 160° was measured in a cylindrical scattering cell (Wells et al., 1986).

During the computer-assisted data acquisition, $I_L - I_R$ and $I_L + I_R$ were recorded separately. The angle dependence of the nonpolarized scattering intensity proportional to $I_L + I_R$ was determined at constant voltages of the photomultiplier tube. In these measurements, the feedback circuit regulating the photomultiplier power supply was bypassed. The magnitude of the scattering cross section can vary by 2 or 3 orders of magnitude as a function of the scattering angle. Thus, as the photomultiplier is scanned through the scattering angle, for a fixed value of the dynode voltage, its output could easily escape out of the region of linear response. To avoid this nonlinearity, the measurements were carried out in piecewise angle intervals by resetting the dynode voltage at each interval to a value appropriate to keep the output of the detector within its linear response range. The anode current and the intensity of the light incident on the photocathode were regulated by the feedback circuit and neutral density filters set in front of the photocathode. CIDS measurements were carried out either by following the same protocol or by using the feedback circuit. However, neutral density filters were used in the forward directions, where the intensity of the scattered light was very high.

All measurements were carried out at room temperature. The experimental data presented are mean values obtained from three to five independent experiments. Artifacts, due to ellipticity of the incident beam and multiple scattering, were minimized, and the optimal concentration range of the suspension was adjusted as described earlier (Wells et al., 1986). The base line for CIDS measurements was determined with a suspension of polystyrene spheres. The CIDS ratio values obtained varied between about -2×10^{-4} and $+2 \times 10^{-4}$.

Results and Discussion

The nonpolarized scattering of chloroplast thylakoid membranes exhibits a "smooth", nonstructured angle dependence with the preponderance of forward scattering and a minimum around 120° (Figure 1). A comparison with model calculations for Mie scatterers (pigmented spheres) shows that the angular scattering intensity functions obtained in chloroplasts resemble that of a sphere with a diameter of about 500 nm [cf. Kerker (1969)]. This suggests, in agreement with an earlier proposal based on the analysis of selective light scattering of mesophyll and bundle sheath chloroplasts of maize (Bialek et al., 1977), that the most intense source of scattering in chloroplasts is the grana.

CIDS ratio exhibits a more complex angular pattern than the nonpolarized scattering. The angle dependence of CIDS and that of the nonpolarized scattering appear entirely unrelated to each other. Furthermore, CIDS, as a function of scattering angle, displays intense lobes with alternating signs (Figure 2).

These results provide unequivocal experimental evidence that differential scattering plays a very important role at 514.5 nm (i.e., around the major short-wavelength CD band). Involvement of light scattering in the anomalous CD signal of chloroplasts was first recognized by Philipson and Sauer (1973), who suggested that contribution of differential scattering to the measured CD spectra of chloroplasts was substantial. Later, this conclusion was challenged by systematic studies of differential scattering in chloroplasts. Although intense circular differential scattering signals were detected between 600 and 740 nm in the forward direction (Gregory & Raps, 1974) and at 90° (Fauldi-Daniel et al., 1978), it was concluded that CIDS did not significantly perturb the CD spectrum recorded in a conventional polarimeter. The corrections were carried out with the basic assumption that the contribution of differential scattering effects to the CD signal was proportional to the relative intensity of nonpolarized scattering. This assumption has been proven erroneous (Bustamante et al., 1983). (In particular, see eq 3–5 of this reference.) Another misleading experimental finding (Faludi-Daniels et al., 1978) is that the differential scattering signals of chloroplasts at right angles from the incident direction are of opposite sign to that of the CD signal. These authors concluded erroneously that the differential scattering signals were unrelated to the circular dichroism signals and could not affect each other. It has been shown that this is not the case (Bustamante et al., 1983).

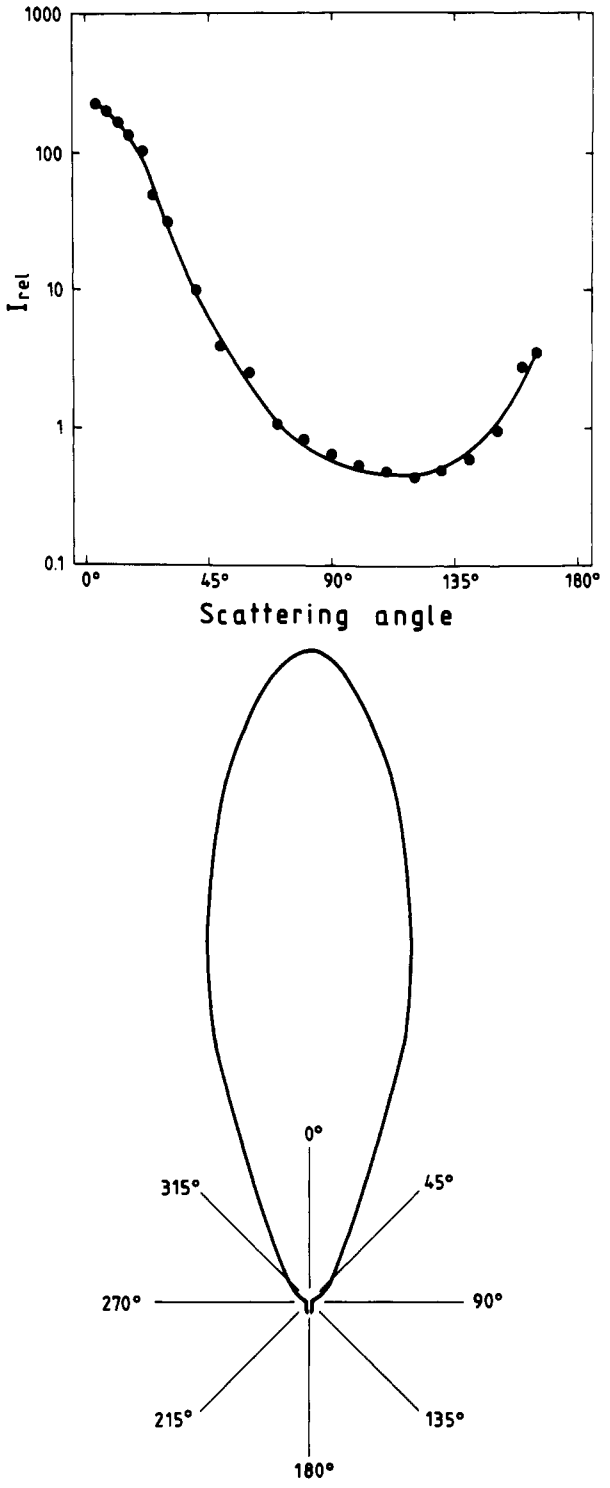

FIGURE 1: Angle dependence of nonpolarized scattering in chloroplast thylakoid membranes (upper) and the corresponding polar plot (lower). (Because of symmetry, the polar plot was also drawn between 180° and 360°.) The chlorophyll concentration of the suspension was adjusted to 15 and 5 μM in the rectangular and the cylindrical cells, respectively (cf. Experimental Procedures).

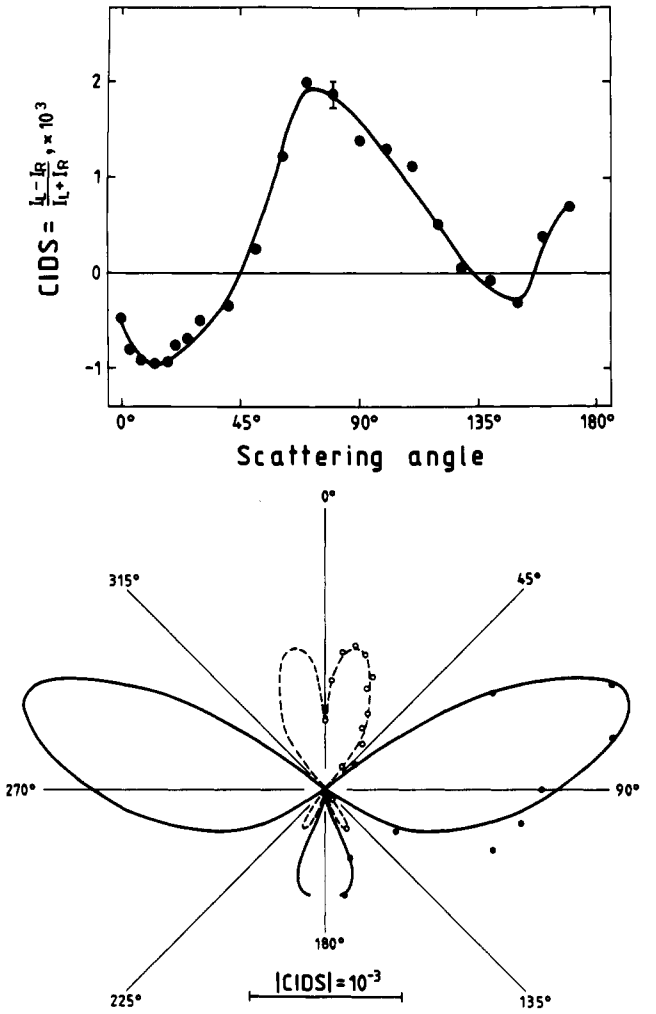

FIGURE 2: Angle dependence of CIDS in chloroplast thylakoid membranes (upper) and the corresponding polar plot (lower). Error bar is marked at 80°. Dashed and solid lines in the polar plot correspond to negative and positive CIDS values, respectively. (For further details, see Figure 1 and Experimental Procedures.)

In retrospect, these experimental results can be reconciled with the original notion of Philipson and Sauer (1973) and a more recent suggestion (Garab et al., 1988a) that differential scattering and very likely a ψ-type CD phenomenon closely associated with CIDS (Keller & Bustamante, 1986) play an important role in defining the characteristics of the CD of chloroplasts. It is now well established that nonpolarized scattering and CIDS carry distinct physical information about the architecture of the scattering substance (Bustamante et al., 1980, 1982). The angle dependence of the CIDS ratio and that of nonpolarized scattering are entirely unrelated to each other. It has also been predicted by the CIDS theory and observed experimentally in different helically organized biological structures (Tinoco et al., 1987) that CIDS, as a function of scattering angle, displays intense lobes with alternating signs.

Our experimental findings—independence of the angular intensity patterns of CIDS and nonpolarized scattering and the presence of alternating lobes in the angle dependence of CIDS (Figures 1 and 2)—are in perfect harmony with the earlier experimental results (Maestre et al., 1982; Wells et al., 1986) and with the predictions of CIDS theory. This permits us to conclude that chloroplasts contain helically organized macroaggregates with dimensions commensurate with the wavelength of the light where CIDS is observed.

The lower limit of particle diameter for which CIDS, at 515 nm, is presumed to apply is more than 25 nm (larger than $^1/_{20}$ of the wavelength). As discussed in detail elsewhere (Garab et al., 1988a,b), circumstantial evidence points to the role of the light harvesting chlorophyll *a*/*b* pigment–protein complex (LHC II) in defining the macrohelical array. Correlations were found between the CD characteristics, the diamagnetic and electric properties of the liquid-crystalline state of the isolated aggregated LHC II, and the same parameters in chloroplasts of high LHC II content (Faludi-Daniel &

Mustardy, 1983; Garab, 1987). This chlorophyll a/b complex, due to its high self-assembly capacity and role in mediating stacking between the thylakoid membranes (Kuhlbrandt, 1984; Staehelin, 1986), may constitute the backbone of the helically organized macrodomains in the thylakoid membranes of grana.

In general, when studying complexes and heterogeneous systems such as chloroplasts, one must be aware of the fact that the structures responsible for most of the nonpolarized scattering cross section may not be the same as those chiral structures responsible for the preferential scattering of the circular polarizations.

Therefore, we carried out CIDS model calculations to fit the experimental results. We modeled only the numerator ($I_L - I_R$) of the CIDS ratio and divided it by the experimental unpolarized scattering ($I_L + I_R$).

The position, sign, and number of lobes in the CIDS pattern are sensitive indicators of the sense of handedness and the dimensions of the chiral structure relative to the wavelength of light (Bustamante et al., 1985). Various chiral models have been described in the literature [simple helices (Bustamante et al., 1982), twisted ladder model (Keller et al., 1985), supercoiled structures (Patterson et al., 1986), etc.]. In all these models, the above conclusions remain valid. Thus, for the calculations performed in this paper, we have chosen a simple helix of defined pitch, radius, and handedness composed by an array of uniaxially polarizable groups. This choice was made for simplicity. The actual magnitude of the scattering lobes appears to depend more on the geometrical detail of the chiral unit, and their prediction requires more sophisticated and detailed models.

The expressions utilized were those obtained for rotationally averaged structures and published elsewhere (Bustamante et al., 1982). Our results indicate that a left-handed helix, with radius and pitch of 385 nm, produces the same number of CIDS lobes of the same sign and the same scattering angle as those observed in the experimental results. This suggests that the LHC II are organized in left-handed helical domains of 385 nm and that these domains are the ones responsible for the preferential scattering of circularly polarized light at 514.5 nm. On the other hand, the overall dimensions of the grana in which these domains are located would be mainly responsible for the nonpolarized scattering.

The results arrived at, although preliminary, can be thought of as a first approximation of the dimensions and geometry of the chiral domains. Uncertainty in the presence of the backscattering lobe could reduce the dimensions of the left-handed chiral structure to $\sim$200 nm. We can state with certainty that the chiral structures involved have dimensions between 200 and 400 nm.

The dimensions of these chiral centers suggest that the chiral organization of the LHC II involves nearly the whole extent of the grana structure. It is expected that the grana structure is retained in the suspension of C-chloroplasts, since Garab et al. (1988a) have shown that C-chloroplasts prepared in the same way as in this work have identical CD signals to those of A-chloroplasts.

These chiral macroarrays are most likely identical with the large domains detected by fluorescence yield measurements following picosecond excitation of chloroplasts (Geacintov & Breton, 1986). It appears that the pigments are organized into large domains with the reaction centers embedded in the lake of bulk pigments. This model is often called "lake model". No a priori restriction is implied on the rotational mobility of the constituent pigment protein complexes in this model. We have found evidence for the existence of a macrohelical array of the pigment–protein complexes. This macrohelicity requires that the rotational freedom of the complex be somewhat restricted.

It is not possible yet to propose a detailed model for the structural organization of the LHC II in the thylakoid of the grana. To carry out this program, we plan to continue experiments along the direction mentioned above and to use more sophisticated model calculations. Our results also demonstrate the usefulness of CIDS to detect chiral organizations in the study of complex polydisperse biological structures, such as chloroplasts. This sensitive, nondestructive technique, which is unique in its capability of detecting chiral macroaggregates in biological systems, may also prove useful in studying the dynamics and nature of ultrastructural changes in response to physiochemical or environmental conditions.

References

Bialek, G. E., Horvath, G., Garab, Gy. I., Mustardy, L. A., & Faludi-Daniel, A. (1977) *Proc. Natl. Acad. Sci. U.S.A. 74*, 1455–1457.

Breton, J., & Nabedryk, E. (1987) in *The Light Reactions* (Barber, J., Ed.) pp 159–195, Elsevier, Amsterdam.

Bustamante, C., Maestre, M. F., & Tinoco, I., Jr. (1980) *J. Chem. Phys. 73*, 6046–6055.

Bustamante, C., Tinoco, I., Jr., & Maestre, M. F. (1982) *J. Chem. Phys. 76*, 3440–3446.

Bustamante, C., Tinoco, I., Jr., & Maestre, M. (1983) *Proc. Natl. Acad. Sci. U.S.A. 80*, 3568–3572.

Bustamante, C., Maestre, M. F., & Keller, D. (1985) *Biopolymers 24*, 1595–1612.

Chylla, R. A., Garab, Gy., & Whitmarsh, J. (1987) *Biochim. Biophys. Acta 894*, 562–571.

Faludi-Daniel, A., & Mustardy, L. A. (1983) *Plant Physiol. 73*, 16–19.

Faludi-Daniel, A., Bialek, G. E., Horvath, G., Sz-Rozsa, Zs., & Gregory, R. P. F. (1978) *Biochem. J. 174*, 647–651.

Garab, G. (1987) *Mol. Cryst. Liq. Cryst. 152*, 259–266.

Garab, G., Szito, T., & Faludi-Daniel, A. (1987) in *The Light Reactions* (Barber, J., Ed.) pp 305–339, Elsevier, Amsterdam.

Garab, G., Faludi-Daniel, A., Sutherland, J. C., & Hind, G. (1988a) *Biochemistry 27*, 2425–2430.

Garab, G., Leegood, R. C., Walker, D. A., Sutherland, J. C., & Hind, G. (1988b) *Biochemistry 27*, 2430–2434.

Geacintov, N. E., & Breton, J. (1986) in *Photosynthesis III: Photosynthetics Membranes* (Arntzen, C. J., & Staehelin, L. A., Eds.) pp 310–318, Springer-Verlag, Berlin.

Gregory, R. P. F., & Raps, S. (1974) *Biochem. J. 142*, 193–201.

Hall, D. O. (1972) *Nature (London), New Biol. 235*, 125–126.

Hall, K., Wells, K. S., Keller, D., Samori, B., Maestre, M. F., Tinoco, I., Jr., & Bustamante, C. (1985) in *Applications of Circularly Polarized Radiation* (Allen, F. S., & Bustamante, C., Eds.) pp 77–91, Plenum, New York.

Katz, J. E., Wells, K. S., Ussery, D., Bustamante, C., & Maestre, M. F. (1984) *Rev. Sci. Instrum. 55*, 1574–1579.

Keller, D., & Bustamante, C. (1986) *J. Chem. Phys. 84*, 2972–2980.

Keller, D., Bustamante, C., Maestre, M. F., & Tinoco, I., Jr. (1985) *Biopolymers 24*, 783–797.

Kerker, M. (1969) *The Scattering of Light and Other Electromagnetic Radiation*, Chapter 4.4.2, pp 161–172, Academic, New York.

Kühlbrandt, W. (1984) *Nature (London) 307*, 478–480.

Maestre, M. R., Bustamante, C., Hayes, T. L., Subirana, I. A., & Tinoco, I., Jr. (1982) *Nature (London) 298*, 773–774.

Maestre, M. F., Salzman, G. C., Tobey, R. A., & Bustamante, C. (1985) *Biochemistry 24*, 5152–5157.
Michel, H., & Deisenhofer, J. (1986) in *Photosynthesis III: Photosynthetic Membranes* (Arntzen, C. J., & Staehelin, L. A., Eds.) pp 371–381, Springer-Verlag, Berlin.
Patterson, C. W., Singham, S. B., Salzman, G. C., & Bustamante, C. (1986) *J. Chem. Phys. 84*, 1916–1921.
Philipson, K. D., & Sauer, K. (1973) *Biochemistry 12*, 535–540.
Staehelin, L. A. (1986) in *Photosynthesis III: Photosynthetic Membranes* (Arntzen, C. J., & Staehelin, L. A., Eds.) pp 1–84, Springer-Verlag, Berlin.
Tinoco, I., Jr., Maestre, M. F., & Bustamante, C. (1983) *Trends Biochem. Sci. (Pers. Ed.) 8*, 41–44.
Tinoco, I., Jr., Mickols, W., Maestre, M. F., & Bustamante, C. (1987) *Annu. Rev. Biophys. Biophys. Chem. 16*, 319–349.
Wells, K. S., Beach, D. A., Keller, D., & Bustamante, C. (1986) *Biopolymers 25*, 2043–2064.
Zuber, H., Brunisholz, R., & Sidler, W. (1987) in *Photosynthesis* (Amesz, J., Ed.) pp 233–271, Elsevier, Amsterdam.

Articles

Membrane Potential Modulates Photocycling Rates of Bacterial Rhodopsins†

Danny Manor, C. A. Hasselbacher, and John L. Spudich*
Department of Anatomy and Structural Biology, Albert Einstein College of Medicine, Bronx, New York 10461
Received November 17, 1987; Revised Manuscript Received March 16, 1988

ABSTRACT: Effects of membrane potential on photochemical reactions of three retinal-containing chromoproteins in *Halobacterium halobium*, sensory rhodopsin I (sR-I), bacteriorhodopsin, and halorhodopsin, are described. Each of the three exhibits a decreased rate of thermal decay of its principal intermediate when photoactivated in an artificially energized compared to a deenergized membrane. The similar response of the three pigments suggests a voltage-dependent conformational change common to their respective photocycles. Spectral and kinetic properties of the sR-I photochemical reaction cycle were measured in phototactic *H. halobium* cells, and differences from in vitro photocycle kinetics were attributable to the electrical membrane potential present in vivo. In vivo sR-I photocycling rates were reproduced in envelope vesicle preparations in the presence of a valinomycin-induced potassium diffusion potential.

Four retinal-containing proteins have been found in *Halobacterium halobium* membranes. Bacteriorhodopsin (bR, λ_{max} = 568 nm) and halorhodopsin (hR, λ_{max} = 578 nm) are light-driven ion pumps (for H^+ and Cl^-, respectively) which hyperpolarize the membrane, contributing energy to the cell in the form of transmembrane electrochemical potential [for reviews, see Stoeckenius (1980), Stoeckenius and Bogomolni (1982), and Lanyi (1986)]. In addition, the cells exhibit light-induced motility responses mediated by at least two phototaxis receptors, sensory rhodopsins I and II (sR-I, λ_{max} = 587 nm, and sR-II, λ_{max} = 480 nm) [for recent reviews, see Takahashi et al. (1987) and Spudich and Bogomolni (1988)]. Like bR and hR, the sensory rhodopsins undergo cyclic photochemical reactions, which, however, do not result in membrane hyperpolarization. Both sR-I and sR-II have long-lived photointermediates with absorption maxima in the near-UV. $SR\text{-}I_{587}$ is an attractant light receptor which allows cells to migrate into regions optimal for their light-driven ion pumps. Its long-lived intermediate (S_{373}) and $sR\text{-}II_{480}$ are repellent light receptors.

Biochemical and photochemical properties of sR-I and sR-II have been obtained almost exclusively from measurements using membranes prepared from *H. halobium* cells (Bogomolni & Spudich, 1982; Spudich & Bogomolni, 1983). Recently, a strain has been isolated [Flx5R (Spudich et al., 1986)] which produces the sR-I apoprotein in sufficient quantity to permit investigation of this pigment's photocycle in vivo. In this paper, we describe photocycling of sR-I in intact Flx5R cells under conditions in which they exhibit phototaxis and in sonicated cell envelopes in the presence or absence of electrical potential across the membrane. These results are compared to those obtained with similar vesicles containing bR and hR.

Our studies reveal a modulation of the sR-I photocycle by membrane potential in vivo. Such an effect on sR-I was suggested earlier by the observation that the sR-I photocycle was retarded by photoactivation of hR in the same membrane and that this effect was partially reversed by proton ionophore (R. Bogomolni, personal communication). This result and a similar effect on hR, reported here, generalize the membrane potential modulation of the bR photocycle noted previously from the effects of illumination on bR (Westerhoff & Dancshazy, 1984).

Materials and Methods

Chemicals. 3,3′-Dipentyloxadicarbocyanine iodide [$diOC_5(3)$][1] was purchased from Molecular Probes (Eugene,

† This work was supported by National Institutes of Health Grant R01 GM27750 to J.L.S. C.A.H. was supported by National Institutes of Health Training Grant T32 DK07513.

[1] Abbreviations: CCCP, carbonyl cyanide *m*-chlorophenylhydrazone; TPB, tetraphenylboron; DNP, 2,4-dinitrophenol; HEPES, *N*-(2-hydroxyethyl)piperazine-*N*′-2-ethanesulfonic acid; TRIS, tris(hydroxymethyl)aminomethane; $diOC_5(3)$, 3,3′-dipentyloxadicarbocyanine iodide; $diOC_2(3)$, 3,3′-diethyloxacarbocyanine iodide; $\Delta\Psi$, transmembrane electrical potential; $\Delta\Psi_{K^+}$, valinomycin-induced potassium diffusion potential; $t_{50\%}$, time for recovery of 50% of the initial absorbance change; $t_{1/2}$, half-time for a process obtained from curve fitting of the data to first-order kinetics.

0006-2960/88/0427-5843$01.50/0